International Journal of Engineering Sciences & Research Technology

(A Peer Reviewed Online Journal)
Impact Factor: 5.164

IJESRT

ISSN: 2277-9655
Impact Factor: 5.164
CODEN: IJESS7

IJESRT
INTERNATIONAL JOURNAL OF ENGINEERING SCIENCES & RESEARCH TECHNOLOGY

TWO-DIMENSIONAL MODELLING OF HEAT TRANSFER IN THE WALLS OF A PARALLELEPIPED COLD ROOM: THE CASE OF A TRANSPORTABLE CONTAINER

Hermann KABORE*[1], Roger Mathurin Charles COMPAORE[1,2], Kassoum YAMBA[2], Kalifa PALM[1,2], Oumar SANOGO[1,2]

[1]Université Joseph KI-ZERBO, Unité de Formation et de Recherche en Sciences Exactes et Appliquées (UFR-SEA), Laboratoire d'Energies Thermiques Renouvelables (L.E.T.RE), 03 BP 7021 Ouagadougou, Burkina Faso

[2]Centre National de la Recherche Scientifique et Technologique (CNRST), Institut de Recherche en Sciences Appliquées et Technologies (IRSAT), Laboratoire des Systèmes d'Energie Renouvelable et Environnement-Groupe de Mécanique Industrielle (LASERE-GMI), 03 BP 7047 Ouagadougou 03, Burkina Faso

DOI: 10.57030/ijesrt.13.6.1.2024

ABSTRACT

The aim of this work is to carry out a numerical analysis of the radiative, conductive and convective transfers in the walls of a 2D cold room in order to determine the temperature variation from outside to inside. The device, powered by photovoltaic solar panels installed above the roof via a refrigeration unit, is adjoined by a technical room. The cold store, including the technical room, measuring 5.10 m × 3.00 m × 2.60 m, rests on concrete blocks some 40 cm above the ground, creating a hollow space. Its main purpose is to reduce rising damp. A program was developed in Matlab software to calculate the global radiation received on each wall, including the roof. Thus, for each month from March to May, we calculated the global flux received by the walls on a typical day of the corresponding month. This report presents the computational simulation model implemented using COMSOL Multiphysics, CFD (Computational Fluids Dynamic) software for thermo-fluid-dynamic simulations. We were able to obtain a maximum temperature of 315 K for the outer face and 280.14 K for the inner face. The results of this numerical analysis are validated with those of the program developed on Matlab

KEYWORDS: cold room, model, temperature distribution, simulation, composite wall

1. INTRODUCTION

Cold stores play a major role in the storage and preservation of products of various varieties. The walls that make up the cold store are the interface between the internal and external environments; they are the seat of heat, humidity, vapour or water content transfers, depending on the type of material. Most of the walls of these chambers are made of composite materials, i.e. multi-layered (Roger, 2019; Sidwaya, 2020). When a cold store's envelope is not well insulated, it can not only cause major damage to the agricultural products stored, but also lead to over-consumption of electrical energy by the refrigeration unit. The cold store envelope must also be made up of a vapour barrier to prevent water vapour from passing through the walls of a cold store due to the difference in vapour pressure inside and outside the walls (Neale et al., 1981). Consequently, controlling heat and water vapour transfer in complex materials is essential not only for characterising the behaviour of structures in terms of durability and waterproofing, but also for accurately assessing thermal and energy performance. The characterisation and numerical study of the thermal behaviour of complex walls have been addressed by many researchers (Roger, 2019, Habiba et al. 2014). However, an appropriate model has not yet been implemented to predict the temperature evolution through multilayer panels. This is due to the complexity of this part of the study, which consists of several heterogeneous layers whose modelling depends on the material chosen.

ISSN: 2277-9655
Impact Factor: 5.164
CODEN: IJESS7

The CFD heat transfer model is proposed by (Liman et al., 2014) on black agglomerated cork, encapsulated by wood, showed good thermal insulation of the composite. The model reveals a temperature gradient across the walls during the passage of heat flow. This model, which is intended to be numerical (COMSOL Multiphysics), does not take into account the transfer of water, humidity and water vapour, which are important thermophysical parameters when choosing materials. Our model is based on local, more accessible materials, including those on the external and internal faces which are non-hygroscopic and form vapour barriers designed to keep out the cold. These are enclosed panels whose insulation, expanded polystyrene, is encapsulated by galvanised steel, the parameters of which are presented in (Neale et al., 1981). The thermophysical transfers studied in our model are based on the principle of conservation of energy.

In the simulation, the inside and outside temperatures of the east and west walls evolve differently over the course of a day. For the east wall, the maximum temperature difference is 34.86 K, while for the west wall it's 33.76 K

2. MATERIALS AND METHOD

Presentation of the 3d physical model

The bioclimatic solar cold room is powered by photovoltaic panels located above the roof. The parallelepipedic cold room is 5.10 m long, 3.03 m wide and 2.60 m high. The adjoining room is fitted with a heat evacuation system to allow heat exchange between the electronic equipment and the outside environment. The six walls of the device are made up of three layers, the central layer being made of expanded polystyrene, thickness e_2 covered on both sides by external and internal galvanised steel of identical thicknesses e_1 and e_3 respectively. The physical model of the photovoltaic solar cold store designed on <<AutoCAD 2015>> software is shown in *Fig.1.* below.

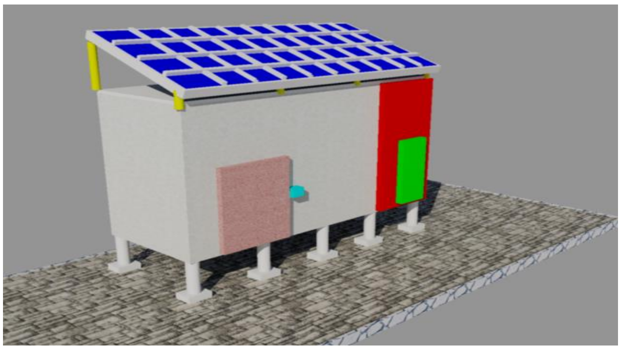

Fig.1. Bioclimatic model of the photovoltaic solar cold room.

Impact of orientation on solar gain

To simulate irradiation, we use the solar flux calculation equations reviewed and proposed by (Dissa, 2007). A program was developed in Matlab language to calculate the global radiation received on each wall, including the roof for typical days (Amadou, 2021) of the tomato conservation months (Hassime, 2018). The equations used to simulate direct, diffuse and global solar radiation on walls and roof are shown below :

$$R_{direct} = (I_O C) \times A \times e^{\left(\frac{-B}{\sin(h)}\frac{P}{1000}\right)} \times \cos(i) \quad (1)$$

$$R_{diffuse} = \left(\frac{1+cos\beta}{2}\right) \times E_H + \left(\frac{1-cos\beta}{2}\right) \times \rho G_H \quad (2)$$

$$R_{global} = R_{direct} + R_{diffuse} \quad (3)$$

Coupled heat transfer modelling

In this work, we have opted for a two-dimensional model based on the conservation of energy equations. It is used to predict the temperature distribution within a complex building material. The model is solved using the finite element method under <<COMSOL Multiphysics>> software. Next, a validation of the model was undertaken by comparing the results obtained with those from the programme developed in Matlab language.
Model assumptions

Heat transfer takes place perpendicular to the walls;

ISSN: 2277-9655
Impact Factor: 5.164
CODEN: IJESS7

Composite walls are assumed to have a homogeneous composition, including the roof and floor;
The fluid is Newtonian and incompressible;
Heat transfer is bidirectional;
The floor and roof of the storage room are assumed to be insulated and impermeable;
The thermo-physical properties of building materials (ρ_s, C_s, λ_s) are constant over time;
On a given surface of the outer and inner wall, the flow of air received at each instant is uniform at all points on this surface.

Mathematical modelling
Governing equations

The general conservation of energy equation for a stationary body with no internal heat source is written (Darrell et al., 2017).

Layer 1 :

$$\frac{\partial}{\partial x}\left(k_{1x}(T_1)\frac{\partial T_1}{\partial x}\right)+\frac{\partial}{\partial y}\left(k_{1y}(T_1)\frac{\partial T_1}{\partial y}\right)=\rho_1 C_{p1}\frac{\partial T_1}{\partial t} \qquad (4)$$

Layer 2 :

$$\frac{\partial}{\partial x}\left(k_{2x}(T_2)\frac{\partial T_2}{\partial x}\right)+\frac{\partial}{\partial y}\left(k_{2y}(T_2)\frac{\partial T_2}{\partial y}\right)=\rho_2 C_{p2}\frac{\partial T_2}{\partial t} \qquad (5)$$

Layer 3:

$$\frac{\partial}{\partial x}\left(k_{3x}(T_3)\frac{\partial T_3}{\partial x}\right)+\frac{\partial}{\partial y}\left(k_{3y}(T_3)\frac{\partial T_3}{\partial y}\right)=\rho_3 C_{p3}\frac{\partial T_3}{\partial t} \qquad (6)$$

Where $k_x(T)$ and $k_y(T)$ are the temperature-dependent thermal conductivities in the x and y directions respectively.

Initial and boundary conditions

$$A\ t_0 \quad T = T_a$$

$$k_{1x}(T_1)\frac{\partial T_1}{\partial x}l + k_{1y}(T_1)\frac{\partial T_1}{\partial y}m + h_{ext}[T - T_{ext}] + \varepsilon\sigma[T^4 - T_{ext}^4] = 0 \quad sur\ S1 \qquad (7)$$

$$k_{2x}(T_2)\frac{\partial T_2}{\partial x}l + k_{2y}(T_2)\frac{\partial T_2}{\partial y}m + q_c = 0 \quad sur\ S2 \qquad (8)$$

$$k_{3x}(T_3)\frac{\partial T_3}{\partial x}l + k_{3y}(T_3)\frac{\partial T_3}{\partial y}m + h_{int}[T - T_{int}] = 0 \quad sur\ S3 \quad (9)$$

Where $S1 \cup S2 \cup S3 = S$ and $S1 \cap S2 \cap S3 = 0$. S is the total area of the domain (m^2). In the above equations $l\ et\ m$ are the direction cosines, h is the convective heat exchange coefficient (W.m^{-2} .K^{-1}), ε is the emissivity of the steel, σ is the Stefan-Boltzmann constant (5.669×10^{-8} W.m^{-2} .K^{-4}), k is the thermal conductivity of the material (W.m^{-1} .K^{-1}) and q_c is the conductive heat transfer (W.m^{-2}).

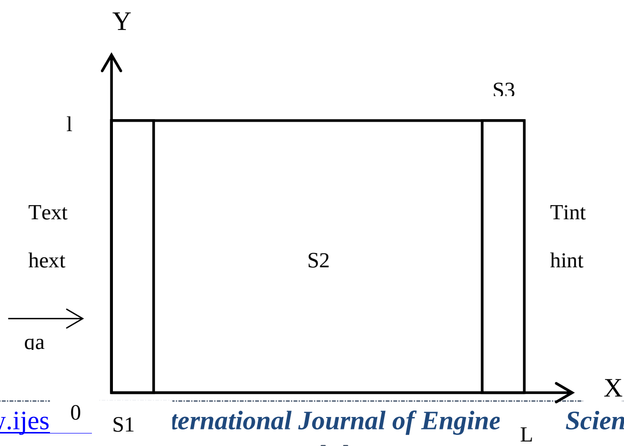

ISSN: 2277-9655
Impact Factor: 5.164
CODEN: IJESS7

Fig.2. 2D physical model of the composite wall

Digital resolution

Equations (4), (5) and (6) together with the boundary conditions form a system of non-linear partial differential equations (due to the presence of the term T^4) and are solved using the finite element method. Galerkin and finite difference methods have been applied to discretise the equations (Roland et al., 2004).

3. RESULTS AND DISCUSSION

Changes in solar irradiance

The variation in hourly solar flux from March to May on the various walls and roof was simulated using equations (1), (2) and (3). We present the results obtained in *Fig.3.* below :

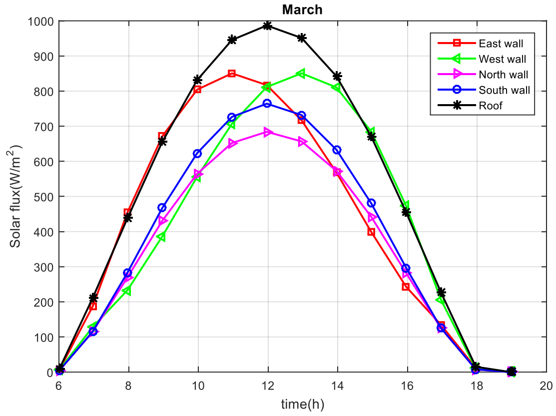

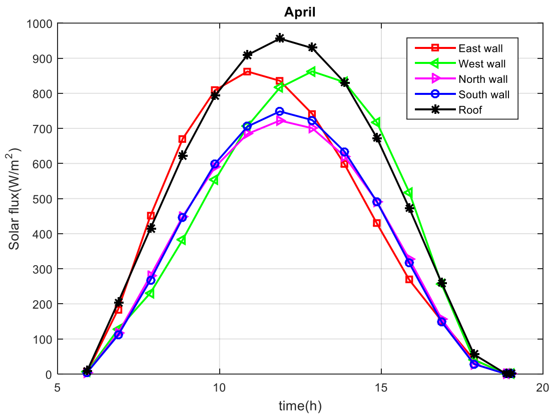

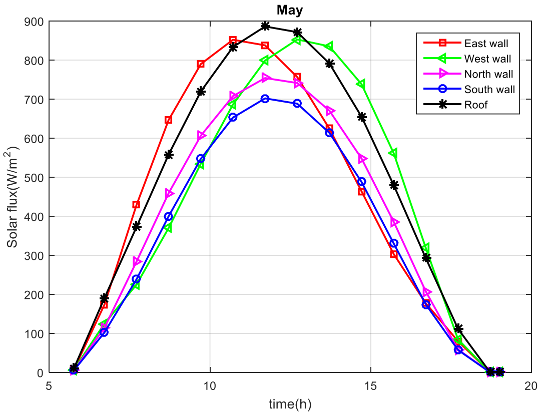

Fig.3: Influence of wall orientation on solar flux from March to August.

From March to May, the maximum fluxes received by the composite walls were observed on the east and west façades at around 11am and 1pm respectively. During this period, the peak solar flux is around 850 W.m^{-2} for both façades, with a phase shift of two (02) hours. This is due to the variation in the sun's path during the different months of the year.

In view of these results, the east and west facades receive the most sunshine during the tomato storage period. As the roof of the cold room is shaded by the photovoltaic solar field, we adopt a good orientation, taking into account the inclination of the photovoltaic panels, to reduce the effect of solar gain.

Numerical simulation

The composite wall studied is that shown in *Fig.2.* The temperature profiles obtained with COMSOL Multiphysics were plotted. The results are shown in the figures below.

Temperature trends in the east walls on a typical day

The walls are subject to thermal disturbance from the sun's rays. This causes their temperatures to vary. The temperature of the east wall is shown in *Fig. 4.*

The temperature on the outside of the east room rises rapidly from 303 K to 315 before dropping to 312 K. This change is normal in that it follows the change in ambient temperature and solar flux over the course of a typical day.

The temperature of the insulating layer drops from 7am to 8am, i.e. from 302 K to 293.8 K, before rising slightly to 298 K at around 3pm. After this time, it drops to 297 K and becomes constant. This variation in the temperature of the insulating layer is due to the fact that it is encapsulated between two walls reaching different temperature peaks.

As for the temperature of the inner surface, it decreases very significantly (from 301 K to 280.14 K) and becomes linear from 1pm onwards. This can be explained by the fact that the cold room enclosure operates at a very low temperature during the day.

The difference between the temperature on the outside and the inside reaches a maximum of 34.86 K. All these findings testify to the insulating capacity of the complex wall.

ISSN: 2277-9655
Impact Factor: 5.164
CODEN: IJESS7

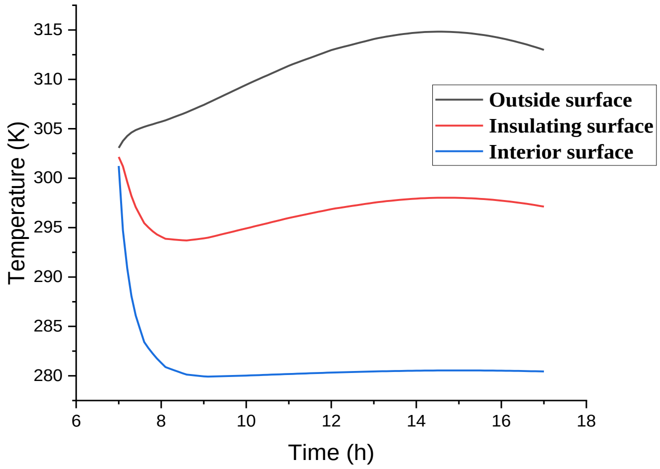

Fig.4. Temporal variation of the temperature on the different layers of the east wall

Temperature trends in the west walls on a typical day

The internal and external temperature trends of the west wall are similar to those of the east wall *Fig.5.* except that they have a slightly smaller amplitude than those of the east wall. As the electronic equipment is located in the adjoining room, close to the east wall, it also contributes to the rise in heat in this wall. The difference between the temperature on the outside and inside is 33.76 K. The three homogeneous layers forming the composite walls are therefore almost insulating.

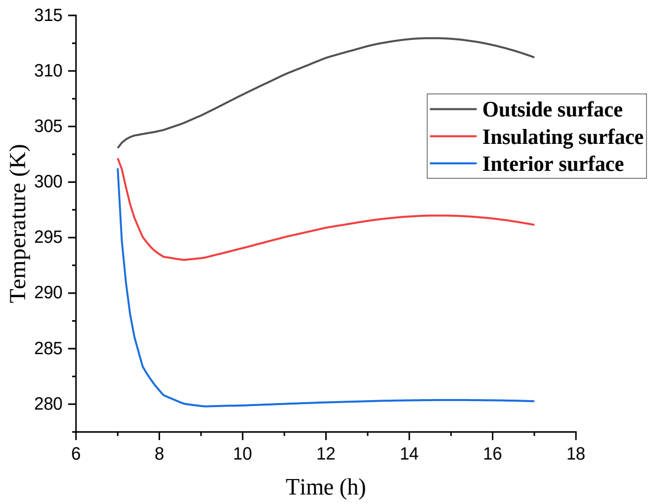

Fig.5. Temporal variation of the temperature on the different layers of the West wall

Evolution of the temperature in the walls on a line cut through the thickness at H = 50 cm

The temperature variations in the wall thickness at different times are shown in *Fig. 6.*

ISSN: 2277-9655
Impact Factor: 5.164
CODEN: IJESS7

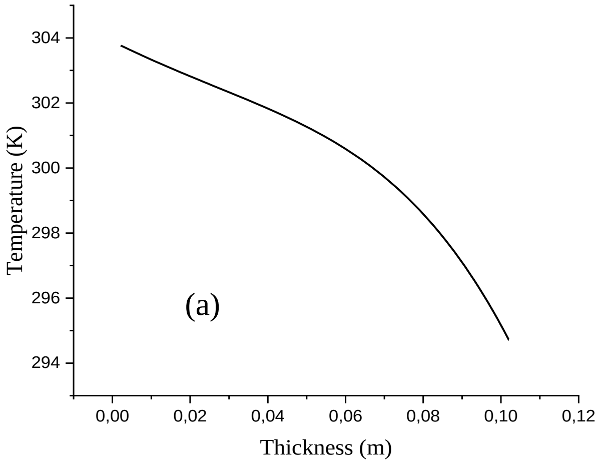

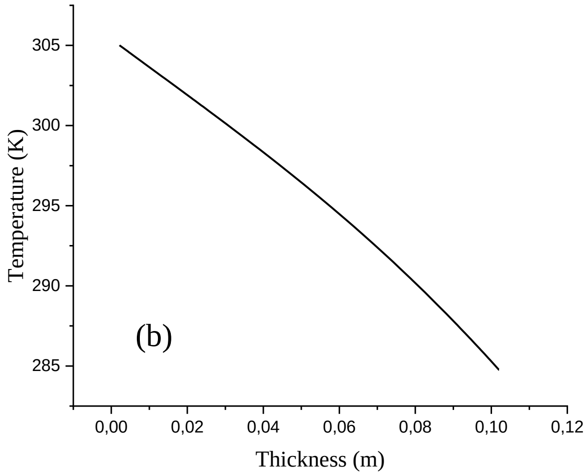

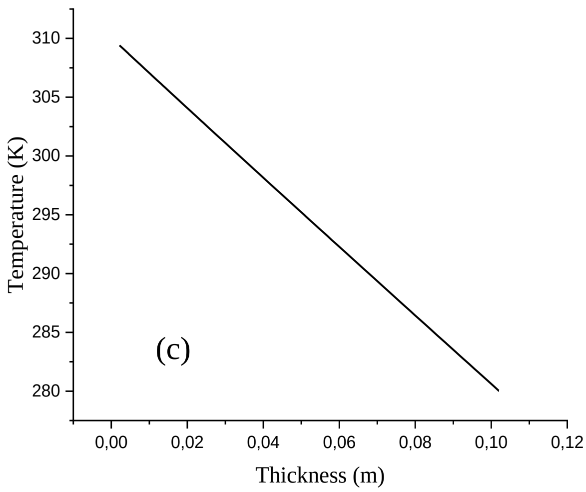

ISSN: 2277-9655
Impact Factor: 5.164
CODEN: IJESS7

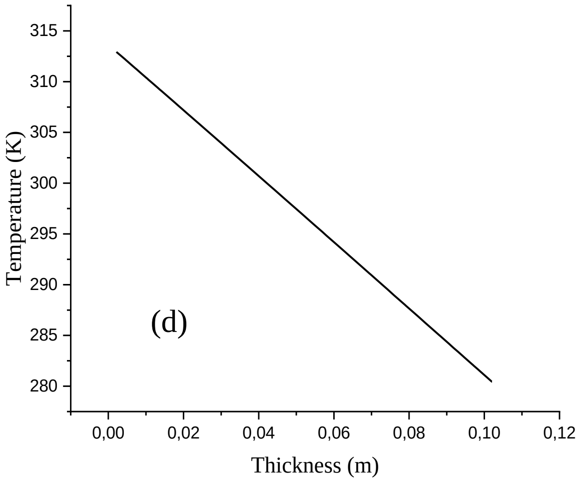

Fig.6. Temperature profiles at H = 50 cm, (a)- 0.1h, (b)- 0.5h, (c)- 2.5h, (d)- 4h

These curves represent the thermal behaviour of the complex wall of the photovoltaic solar cold store after 06 min, 30 min, 2h30mn and 4h of operation. The temperature profiles on these different curves vary as a function of time. At the start of the chiller at 7am, after 0.1h of operation (a), the temperature difference between the external and internal walls is approximately 9.3 K. 30 minutes after operation (b), this difference is 20.3 K. As the cold store is always running without interruption of the electrical current, the internal temperature gradually decreases. The temperature difference between the outer and inner walls is around 28.86 K after 2.5 hours of operation (c). It can be seen that the internal temperature becomes constant and reaches its steady state of approximately 280.14 K after 4 hours of power supply to the chiller. On the other hand, the temperature on the external wall increases due to sunshine, resulting in a temperature difference of approximately 305.86 K (d). It can be seen that the curve becomes linear as the cold room operates, while at the same time the temperature difference between the two composite walls gradually increases. This can be explained by the good insulating capacity of the inner layer on the one hand, and the fact that the two galvanised steel walls reach different temperature peaks on the other.

Validation with the programme developed in matlab

Fig. 7 shows a comparison of temperature profiles between the model developed and the COMSOL Multiphysics numerical simulation tool.

By analysing the thermal behaviour of the various curves, we can see that the differences between the results from the developed programme and those from the simulation tool are very small. The mean square error (Hoang et al., 2014) calculated for this purpose represents 273.19 K

ISSN: 2277-9655
Impact Factor: 5.164
CODEN: IJESS7

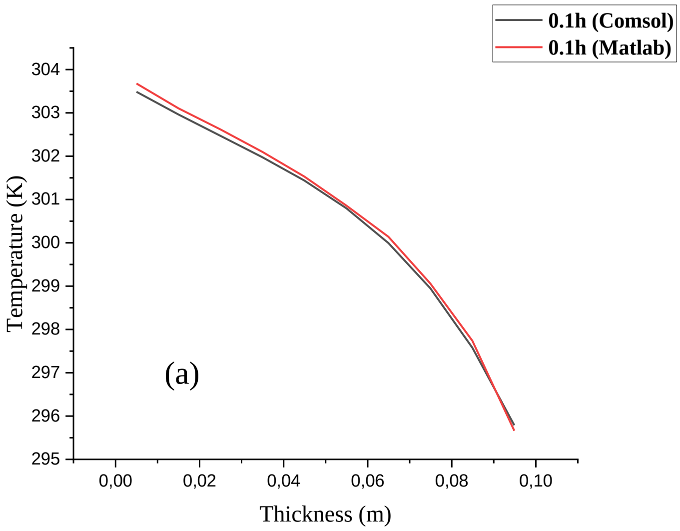

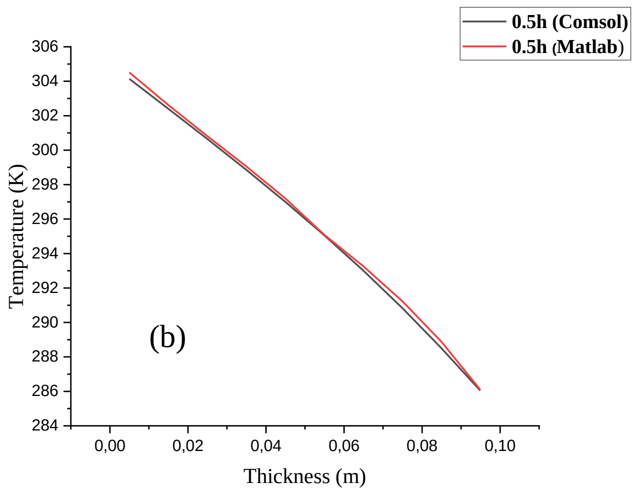

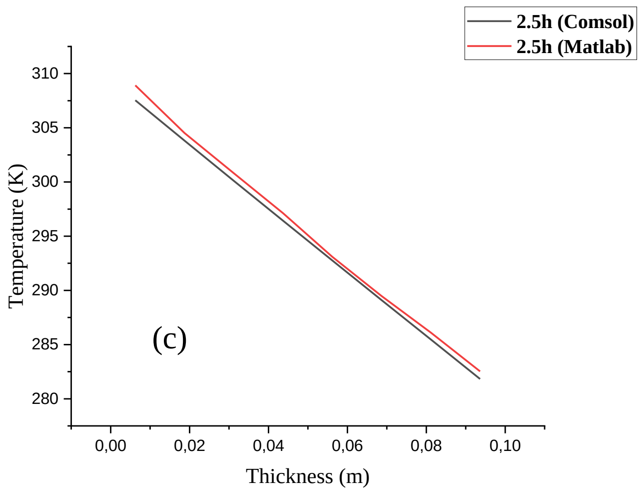

ISSN: 2277-9655
Impact Factor: 5.164
CODEN: IJESS7

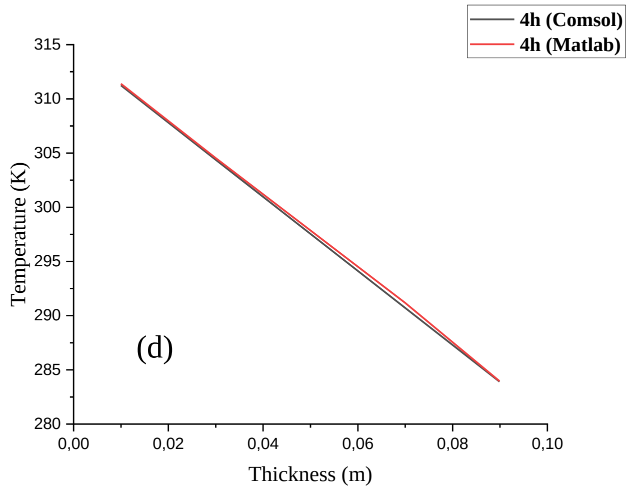

Fig.7. Evolution of the temperature within the wall with the program developed is COMSOL during a typical day, (a)-0.1h, (b)-0.5h, (c)-2.5h, (d)-4h

4. CONCLUSION

This study, which involved modelling heat transfer through complex walls, was carried out on bioclimatic device designed using drawing software. In order to assess the performance of the simulation, a comparison of the results from the different software platforms was undertaken. The comparison of thermal profiles between the developed model and the numerical simulation tool showed slight differences, which are essentially a function of the input parameters chosen for the model. The variation in temperature on the external facade due to sunlight and that on the internal wall imposed by the type of storage of agricultural products have an impact on the thermal behaviour of the composite wall. The greater the temperature difference between the two materials, the more the central insulating layer (expanded polystyrene) has to act as a heat flow barrier to reduce thermal diffusivity. The maximum temperature on the external surface obtained is 315 K and that of the enclosure 280.14 K, giving a temperature difference of 34.86 K. This shows the importance of taking composite walls (galvanised steel-polystyrene-galvanised steel) into account when designing cold rooms for storage and preservation, in order to optimise the energy consumption of the refrigeration unit in terms of thermal insulation.

5. ACKNOWLEDGEMENTS

I would like to thank each co-author for their contribution to the completion of this article, in particular my supervisors Kalifa PALM and Oumar SANOGO. I would also like to thank the Higher Education Support Project (PAES) for their contribution to the payment of the article.

REFERENCES

1. Roger M. C. C. (2019). Conception, réalisation et modélisation d’une chambre froide solaire photovoltaïque pour la conservation des produits agricoles : application au stockage desmangues et de la pomme de terre, Thèse de Doctorat/Université Joseph KI-ZERBO. Physique Appliquée. P.73
2. Sidwaya (2020). Conservation des produits maraîchers : Loumbila/Burkina Faso dispose d’une chambre froide, https://www.sidwaya.info/blog/conservation-des-produits-maraichers-loumbila-dispose-dune-chambre-froide/
3. M. A. Neale & T. Clancey (1981). Transmission hermique et transfert d’humidité au travers des parois d’un entrepôt frigorifique. Bâtiment International, Building Research and Practice, 9:3, 153-161
4. Liman, Amel, Abdel, Zerizer (2014). Modélisation du transfert de chaleur à travers un panneau sandwich destiné à la construction : Cas d’application par COMSOL Multiphysics. COFRET’14-OF1-147. Paris, CNAM-23-24-25

ISSN: 2277-9655
Impact Factor: 5.164
CODEN: IJESS7

5. O. Dissa (2007). Séchage convectif de la mangue : analyse de l'influence des paramètres aérauliques et intrinsèques, conception et modélisation du fonctionnement d'un séchoir solaire indirect. Thèse de doctorat/Université OUAGA 1, Physique, 310 p
6. Amadou O. F. (2021). Impact de la nature des matériaux, de l'orientation et de la ventilation sur le confort thermique dans l'habitat individuel en climat sahélien. Thèse de Doctorat/Université Joseph KI-ZERBO, Physique Appliquée, 45 p
7. Hassime G. (2018). Procédé solaire de production de froid par adsorption (zéolithe-eau) et éléments dimensionnement d'une chambre froide. Thèse de Doctorat/Université Joseph KI-ZERBO. Physique Appliquée. Annexe A, pp. I
8. Darrell W. P. & Juan C. H. (2017). The finite element method. Basic Concepts and Applications with matlab, maple and comsol. series in computational and phtsical processes in mechanics and thermal science. Third edition.
9. Roland W. L., Perumal N., Kankanhally N. S. (2004). Fundamentals of the finite element method for heat and fluid flow, West Sussex PO19 8SQ, England
10. H. M. Hoang, S. Duret, D. flick, O. Laguerre (2014). Preliminary study of airflow and heat transfer in a cold room filled with apple pallets: Comparison between two modelling approaches and experimental results. Applied Thermal Engineering xxx 1-15
11. Roger. M. C. C, Oumar S., Kassoum Y., Ousmane O., Dieudonné J. B. D. (2019). Evaluation of the thermal profile of the solar photovoltaic cold room loaded with mangoes. International Journal of Engineering Sciences & Research Technology, 8 (8), pp. 32-44
12. Habiba K., Abdelghani S., Fares B. Nadjim S., Abdelkader T., Rafik B., Abdelkarim A. M. (2014). Modélisation des transferts de chaleur et de masse dans les parois de bâtiment. ResearchGate/Conference Paper.